ELSEVIER

International Journal of Mass Spectrometry 195/196 (2000) 185–201

International Journal of Mass Spectrometry

Gas-phase reactivity of $SO^{+\cdot}$: a selected ion flow tube study

Brian K. Decker, Nigel G. Adams*, Lucia M. Babcock

Department of Chemistry, The University of Georgia, Athens, GA 30602, USA

Received 8 June 1999; accepted 14 July 1999

Abstract

We present a systematic study of the reactions of $SO^{+\cdot}(X\ ^2\Pi_r)$, an important ion in space plasmas, with organic molecules of interstellar interest. A selected ion flow tube has been used to investigate the reactions of $SO^{+\cdot}$ with CH_4, C_2H_6, C_3H_8, C_2H_2, C_2H_4, C_3H_4 (allene), *n*-C_3H_6, CH_3OH, C_2H_5OH, CH_3OCH_3, OCS, CH_2O, CH_3CHO, $CH_3C(O)CH_3$, HCO_2H, and HCO_2CH_3, and additionally the reactions of $S_2^{+\cdot}$ with C_2H_2 and $O_2^{+\cdot}$ with CH_4, C_2H_2, C_3H_4 (allene), *n*-C_3H_6, CH_3OCH_3, and HCO_2H at 294.5 ± 2.5 K. With just a few exceptions the reactions proceed at or near their theoretical collisional capture rates. Apart from the smaller and more saturated hydrocarbons and OCS, the reactions of $SO^{+\cdot}$ are dominated by heterogenic abstractions of R^- (R = H, OH, CH_3, OCH_3). Charge transfer, where it is exothermic, occurs in competition with the abstraction channels. Hydride abstraction is particularly prevalent, forming the thioperoxy radical, $HSO^{\cdot}$, or its structural isomer, $SOH^{\cdot}$. Hydroxide abstraction to form the hydroxysulfinyl radical, $HOSO^{\cdot}$, occurs in some of the reactions with oxygen-bearing molecules. Where neutral, the abstraction products are inferred from the calculated reaction energetics; however, they are frequently detected directly in their protonated forms. This suggests a two-step reaction mechanism whereby competition for a proton occurs between leaving partners in the exit channel of the activated complex. In the reaction of $SO^{+\cdot}$ with HCO_2CH_3, the protonated methoxysulfinyl radical, $CH_3OSOH^{+\cdot}$, is observed for the first time. The reactions of $SO^{+\cdot}$ with the smaller unsaturated hydrocarbons are more complex, and largely involve rupture of the S–O bond and a C–C bond to form products containing C–S and C–O bonds. The $SO^{+\cdot}$ reactions are discussed in terms of their mechanisms, product formation, thermodynamics, and interstellar significance, and are compared with the related reactions of $S_2^{+\cdot}$ and $O_2^{+\cdot}$. (Int J Mass Spectrom 195/196 (2000) 185–201) © 2000 Elsevier Science B.V.

Keywords: SIFT; SO^+ ion; HSO radical; HOSO radical; Ion/molecule reactions; Hydride ion transfer; Hydroxide ion transfer; Interstellar chemistry

1. Introduction

Oxygen and sulfur are members of the select group of elements which are both cosmically abundant and disposed to forming chemical bonds (chiefly H, O, C, N, Mg, Si, Fe, and S, in decreasing order of solar abundance) [1]. Although sulfur is ranked below Mg, Si, and Fe in abundance, its participation in the ion/molecule chemistry of interstellar clouds is more extensive due to its higher first ionization energy (10.36 eV relative to <8.2 eV for Si, Fe, and Mg); thus, the atomic ions of H, O, C, N, S, and ions derived from these drive the bulk of synthetic gas phase ion/molecule chemistry which directs the chemical evolution of interstellar molecular clouds (ISC) [2–4]. Whereas atomic O^+ does not persist in ISC due

* Corresponding author.

Dedicated to the memory of Robert R. Squires.

1387-3806/00/$20.00 © 2000 Elsevier Science B.V. All rights reserved
PII S1387-3806(99)00146-3

to its rapid reaction with H_2 [5,6], ground-state atomic S^+ is unreactive with both H_2 and CO [5,6], the two major molecular constituents of ISC [2–4]. S^+ in its ground ^4S state is also unreactive with H_2O [5,6]. Sulfur and oxygen in the gas phase in ISC are thought to combine primarily by the ion/molecule reaction

$$S^+ + OH^{\cdot} \rightarrow SO^{+\cdot} + H, \quad (1)$$

which has not yet been studied in the laboratory. Reaction (1) is expected to be particularly important for the synthesis of $SO^{+\cdot}$ in cold, dark interstellar clouds, such as the Taurus Molecular Cloud (TMC-1) [7]. $SO^{+\cdot}$ is one of the 14 sulfur-containing compounds and one of the 13 ions which have been detected in ISC [8].

The sulfur monoxide molecular ion, $SO^{+\cdot}$, itself reacts neither with H_2 nor with CO [6], and thus a consideration of its reactivity with minority species in ISC is necessary. Turner has made the most extensive astrophysical searches for $SO^{+\cdot}$ to date [7,9], and has found this species to be abundant in a wide variety of interstellar sources [7]. His studies were motivated by the potential for $SO^{+\cdot}$ to be a tracer for shocked regions of ISC [7]. In his simple model of $SO^{+\cdot}$ chemistry in ISC, Turner considered electron/ion dissociative recombination to be the only important process that destroys $SO^{+\cdot}$ [9]. His model assumed a recombination rate coefficient of $\alpha_e(SO^{+\cdot}) = 2 \times 10^{-7}\,[T(\mathrm{K})/300]^{-0.5}$ cm^3 molecule^{-1} s^{-1} [9]; a plausible value, albeit one that has not yet been confirmed experimentally. No other destruction pathways for $SO^{+\cdot}$ were considered, which necessitated the assumption of a high electron density (the so-called "high metal" value) to make the chemical model consistent with the observed $SO^{+\cdot}$ column densities in many sources [9]. It is therefore important to investigate whether $SO^{+\cdot}$ can be destroyed by numerous fast ion/molecule reactions with observed and expected interstellar molecules.

From a more fundamental standpoint, the reactivity of $SO^{+\cdot}$ as compared with its isovalent "sister" species, $S_2^{+\cdot}$ and $O_2^{+\cdot}$, is of considerable interest. The most important differences in reactivity among these three species are expected to stem from the essential electronic difference between the component atoms, S and O. The valence electrons of S are better shielded from the nuclear core potential than those of O, and hence, the promotion and ionization energies of electrons in molecular orbitals arising from S atoms are lower than in those arising from O atoms; for the same reason, the electronegativity of S (2.58, Pauling) is substantially lower than that of O (3.44, Pauling) [10]. In consequence, the recombination energies of $S_2^{+\cdot}$, $SO^{+\cdot}$, and $O_2^{+\cdot}$ are 9.36, 10.29, and 12.07 eV, respectively [11], and hence, the capacity for exothermic reaction progresses steadily in the order $S_2^{+\cdot} < SO^{+\cdot} < O_2^{+\cdot}$. For reactions of such ions with polyatomic molecules, the prominence of charge (electron) transfer is also strongly correlated with the charge transfer exothermicity. This is because the high density of rovibronic states available in a polyatomic molecule permits a long-range charge transfer to occur with a high probability of favorable Franck-Condon factors. Here the probability of reaction essentially depends on the volume of phase space available to the reactants, and hence, on the reaction exothermicity. Such charge-transfer mechanisms in ion/molecule reactions have recently been reviewed [12].

As a consequence of the difference in electronegativity between S and O, $SO^{+\cdot}$ is a highly polar species, with an electric dipole moment in the ground $X\ ^2\Pi_r$ state of about 2.2 D [13]; the homonuclear $S_2^{+\cdot}$ and $O_2^{+\cdot}$ clearly lack permanent electric dipole moments. Although the overall collisional capture rates for the reactions of all three ions with neutral molecules will be dominated by the charge/permanent electric dipole and the charge/induced electric dipole interactions [14], the strong dipole of $SO^{+\cdot}$ is likely to distinguish that ion from $S_2^{+\cdot}$ and $O_2^{+\cdot}$ with regard to the intimate reaction mechanisms and the kinds of products formed from the activated complex. Therefore, a comparative study of the reactivities of $S_2^{+\cdot}$, $SO^{+\cdot}$, and $O_2^{+\cdot}$ will investigate the effects of recombination energy and charge separation on the rates and mechanisms of ion/molecule reactions.

Very few reactions of $SO^{+\cdot}$ have been studied previously in the laboratory. The standard ion/molecule reaction databases [5,6] list only eight such

reactions, i.e., with H_2, N, NH_3, O_2, H_2S, CO, SO_2, and SF_6. Four of these, i.e., with H_2, O_2, CO, and SO_2, do not proceed under standard conditions [6]. In contrast, many ion/molecule reactions of $S_2^{+\cdot}$ [5,6,15–18] and $O_2^{+\cdot}$ [5,6,19–25] have been investigated, and hence are available for direct comparison with those of $SO^{+\cdot}$. In the present work, a selected ion flow tube (SIFT) has been used in the first systematic study of the ion/molecule reactions of $SO^{+\cdot}$ with 16 organic molecules identified or likely to be present in ISC [8]: CH_4, C_2H_6, C_3H_8, C_2H_2, C_2H_4, C_3H_4 (allene), *n*-C_3H_6, CH_3OH, C_2H_5OH, CH_3OCH_3, OCS, CH_2O, CH_3CHO, $CH_3C(O)CH_3$, HCO_2H, and HCO_2CH_3. For completeness of comparison, the reactions of $S_2^{+\cdot}$ with C_2H_2 and $O_2^{+\cdot}$ with CH_4, C_2H_2, C_3H_4 (allene), *n*-C_3H_6, CH_3OCH_3, and HCO_2H have also been investigated (of these, only the reactions of O_2^+ with CH_4 and HCO_2H have been studied previously under thermal conditions [5,6,20]). Rate coefficients and product distributions are presented for the reactions of all three ions with the 16 molecules, and the relative reactivities of $S_2^{+\cdot}$, $SO^{+\cdot}$, and $O_2^{+\cdot}$ are discussed in light of these results. For $SO^{+\cdot}$, the reaction mechanisms, nature of the products formed, and implications for chemistry in ISC are also discussed.

2. Experimental

The SIFT technique has been described at length elsewhere [26]; the essentials are presented here, with emphasis on details particular to the present experiments. The $SO^{+\cdot}$ ions were efficiently generated by two methods: (a) directly by impact of 70 eV electrons on SO_2 in a low-pressure ion source (LPIS); and (b) by generation of S^+ from 70 eV electron impact on CS_2 in the same source, followed in the flow tube by

$$S^+(^4S) + O_2(X\ ^3\Sigma_g^-) \xrightarrow{k_2^{(2)}} SO^{+\cdot}(X\ ^2\Pi_r) + O(^3P) + 6.9\ \text{kcal mol}^{-1} \quad (2)$$

where $k_2^{(2)} = 1.8 \times 10^{-11}$ cm^3 molecule^{-1} s^{-1} [6]. In method (b), 100.0 STP cm^3 s^{-1} of O_2 was introduced into the flow tube ~20 cm downstream from the venturi inlet for the He carrier gas; $SO^{+\cdot}$ is not significantly depleted by reaction with O_2 [6]. The indicated exothermicity of reaction (2) (calculated from data available in [11]) is sufficient only to populate the $v \leq 1$ vibrational levels of the ground state ($X\ ^2\Pi_r$) of $SO^{+\cdot}$, and cannot access its electronically excited states [27]. Thus, method (b) was superior to (a) for generating $SO^{+\cdot}$ because the ion was formed with little or no internal excitation, and also because the SO_2 source gas for method (a) aggressively attacked the hot thermionic filament in the ion source, necessitating a filament replacement after every one or two reaction studies. Furthermore, some 90 cm of flow tube lay between the "endpoint" of reaction (2) in the flow tube (defined here as the point at which $[S^+]$ had decayed to e^{-5}, or ~0.7%, of its initial value) and the reactant inlet used in these studies. In this region each $SO^{+\cdot}$ ion experienced ~4×10^4 collisions with the He carrier gas, and additionally ~200 collisions with O_2, which at least partially relaxed any remaining vibrational excitation in $SO^{+\cdot}$ through *V*–*T* and *V*–*V* processes, respectively (see, e.g. discussions in [28]). For these reasons, all of the reactions were studied with $SO^{+\cdot}$ generated by method (b) in the present study.

Although some metastable S^+* (^2P and ^2D) was injected into the flow tube along with $S^+(^4S)$ in method (b), it has been shown that this S^+* reacts with O_2 entirely by charge transfer and collisional de-excitation, generating $O_2^{+\cdot}$ and $S^+(^4S)$, respectively [29]. The $S^+(^4S)$ clearly contributed to the $SO^{+\cdot}(X\ ^2\Pi_r)$ signal by reaction (2), and the O_2^+ appeared as a minor contaminant ion typically at ~6%–8% of the $SO^{+\cdot}$ signal. Fortunately, many of the reactions of $O_2^{+\cdot}$ with the molecules in the present study have been investigated by other workers [5,6,19–25], and their results were used to make small corrections to the product distributions for the contribution from $O_2^{+\cdot}$ reactions. In cases where no data are available in the literature, and in some cases where the available data are inconsistent, (i.e. with C_2H_2, C_3H_4 (allene), *n*-C_3H_6, CH_3OCH_3, and HCO_2H), the reac-

tions of $O_2^{+\cdot}$ were studied by injecting $CO^{+\cdot}$ generated from CO in the same LPIS, followed by a reaction in the flow tube with a 100.0 STP $cm^3\ s^{-1}$ flow of O_2 introduced exactly as described previously:

$$CO^{+\cdot} + O_2 \xrightarrow{k_3^{(2)}} O_2^{+\cdot} + CO \quad (3)$$

where $k_3^{(2)} = 1.5 \times 10^{-10}$ cm^3 $molecule^{-1}$ s^{-1} [6]. In this case, the numerous collisions of $O_2^{+\cdot}$ with O_2 in the flow tube prior to injection of the neutral reactant were expected to efficiently quench, via resonant charge transfer, any metastable $O_2^{+\cdot}$* that may have been formed initially.

To complete the data set for reactions of the three related ions $XY^{+\cdot}$ (X, Y = S, O) with the neutral molecules in this study, the reaction of $S_2^{+\cdot}$ with C_2H_2 was studied with $S_2^{+\cdot}$ generated from OCS in the flow tube as described previously [15].

The precursor ions S^+ and $CO^{+\cdot}$ used in these studies were generated in the LPIS as noted above, guided into the SIFT quadrupole mass filter by a series of ion lenses, selected from amongst the other ions generated in the source, and focused by a second series of ion lenses into the higher-pressure flow tube through a 1.0 mm hole centered in a molybdenum disk electrode. The initial ions of interest were generated by reaction of the precursor ions with O_2 or OCS in the flow tube as noted above, and then reacted with the neutral molecules which were introduced at a ring-type inlet ~90 cm downstream from the region of initial ion synthesis.

The O_2 and OCS flows were maintained by means of a standard calibrated flow meter (MKS), and the flow rates of the other reactants were determined from their initial pressures and pressure drops across a calibrated capillary tube (using the Poiseuille equation). Gas and vapor viscosities needed for this flow determination were obtained from the Yaws handbook [30]. Chemically pure gases were obtained from commercial sources and used without further purification. High performance liquid chromatography grade liquid reagents, also obtained from commercial sources, were further purified by several freeze–pump–thaw cycles before use. The purities of the reagents as quoted by the manufacturers were as follows: CH_4 (99.99 mol %), C_2H_6 (99.0+ mol %), C_3H_8 (99.5 mol %), C_2H_2 (99.6 mol %), C_2H_4 (99.5 mol %), C_3H_4 (allene) (97 mol %), *n*-C_3H_6 (99+ mol %), CH_3OH (99.9+ wt %), C_2H_5OH (200.0 proof), CH_3OCH_3 (99.87 mol %), OCS (97.5+ mol %), CH_2O (paraformaldehyde, 95 wt %), CH_3CHO (99.4 wt %), $CH_3C(O)CH_3$ (99.90 wt %), HCO_2H (99.4 wt %), and HCO_2CH_3 (99.35 wt %). Reagents were used neat except for C_2H_2, which was prepared in a 10% manometric mixture with 5.0 grade Ar, and HCO_2H, which was prepared in a 2.5% manometric mixture with 4.7 grade He that had been cleaned by passing through a liquid nitrogen-cooled molecular sieve trap. The viscosity of the C_2H_2/Ar mixture was estimated using the Brokaw extension of Chapman-Enskog theory [31] along with available values for the viscosities of C_2H_2 [30] and Ar [32]. Because of the small partial pressure of HCO_2H in He, it was justifiably assumed that the viscosity of the mixture was equal to the viscosity of He within a negligible error. However, for accurate determination of HCO_2H throughput, it was necessary to correct for the shift in the monomer/dimer equilibrium of this reagent upon dilution using the data of Taylor and Bruton [33]. Formaldehyde monomer was introduced into the flow line from a flask containing a sample of paraformaldehyde maintained at a temperature of ~110 °C.

All experiments were performed at 294.5 ± 2.5 K in He carrier gas at ~0.5 Torr with a plug flow velocity of ~8000 cm s^{-1}; due to ion diffusion effects [26], the average ion velocity was rather higher at ~12 000 cm s^{-1} [34]. Carrier He flow was established and measured by a calibrated mass flow controller (MKS), and evacuated by a high-capacity Roots-type blower (Stokes). Reactant and product ions were sampled through a 0.3 mm hole in a molybdenum disk electrode situated in a nose cone downstream, separating the flow tube from the differentially pumped downstream mass spectrometer housing. Ions were mass selected by a quadrupole mass spectrometer (Extrel) and detected by an on-axis channel electron multiplier (Detech). Ion signals were then amplified and processed by a gated pulse counter

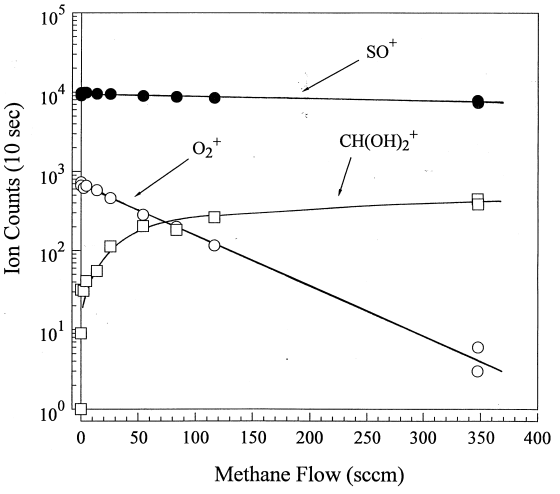

Fig. 1. Variation of $SO^{+\cdot}$, $O_2^{+\cdot}$, and ion product count rates with CH_4 flow. The $O_2^{+\cdot}$ contaminant ion signal is 7% of the $SO^{+\cdot}$ signal. $SO^{+\cdot}$ is unreactive out to a very large flow of CH_4. $O_2^{+\cdot}$ reacts slowly to form $CH(OH)_2^+$, which has been observed previously (see text). The rate coefficient for the $O_2^{+\cdot}$ reaction with CH_4 as determined from this decay plot is in excellent agreement with the previous literature value (see text, Tables 1 and 2, and [6]).

(Stanford Research Systems) and desktop computer. Reaction rate coefficients and product distributions were determined in the usual manner [35,36]. Rate coefficients are estimated to be accurate to ±20% for permanent gases and ±30% for "sticky" vapors and mixtures; reproducibility was consistently ±10% or better. Because all observed primary products occurred in the 26–80 *m/z* range, where the ion detection sensitivity is essentially flat for our system, it was generally unnecessary to correct for mass discrimination; when it was necessary, such a correction could be made by the method we have employed previously [15]. Small corrections to the product distributions for isotopic contributions from neighboring ions, particularly from the ^{34}S and the ^{13}C isotopes, were sometimes necessary. Product distributions are estimated to be accurate to ±5%. Note that this places some uncertainty on the existence of product channels reported with a contribution of <5% to the total product spectrum.

Fig. 1 and Fig. 2(a) and (b) illustrate the typical quality of data collected in this study. In Fig. 1 is a rate plot showing the nonreaction of $SO^{+\cdot}$ with

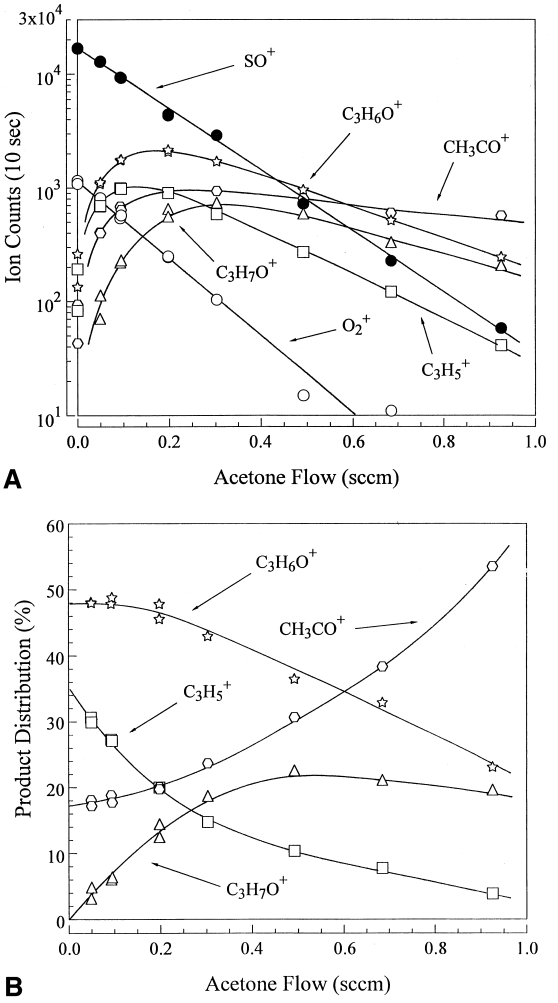

Fig. 2. (a) Variation of $SO^{+\cdot}$, $O_2^{+\cdot}$ and ion product count rates with $CH_3C(O)CH_3$ (acetone) flow and (b) percentages of major (>2%) ion products of the $SO^{+\cdot}$ reaction as a function of acetone flow. In (a), the $O_2^{+\cdot}$ contaminant ion signal is 6% of the $SO^{+\cdot}$ signal. The $SO^{+\cdot}$ decay is linear over more than two orders of magnitude. The apparent falloff in total ion signal with increasing acetone flow is due to secondary and higher-order products which were not monitored (see text). By extrapolation to zero flow in (b), it can be seen that three major (>2%) primary ion products occur in the reaction of $SO^{+\cdot}$ with acetone. The product $C_3H_7O^+$, which is probably $CH_3C^+(OH)CH_3$, or protonated acetone, extrapolates to zero at zero flow, showing it to be a secondary product.

methane, along with the reaction of $O_2^{+\cdot}$ with methane to form $CH(OH)_2^+$, which has been studied previously [5,6]. The $O_2^{+\cdot}$ contaminant appeared at 7% of the $SO^{+\cdot}$ ion signal in this particular study. A bimolecular rate coefficient for the $O_2^{+\cdot}$ reaction of 5.8×10^{-12}

cm^3 $molecule^{-1}$ s^{-1} was obtained from a least-squares fit of the $O_2^{+\cdot}$ signal decay due to this reaction, in excellent agreement with the literature value of 6.0×10^{-12} cm^3 $molecule^{-1}$ s^{-1} ± 15% [6]. All other $O_2^{+\cdot}$ reactions were studied with $O_2^{+\cdot}$ synthesized from $CO^{+\cdot}$ as described above. Fig 2(a) is a rate plot showing the excellent linearity of $SO^{+\cdot}$ decay over more than two orders of magnitude in reaction with acetone. Here the $O_2^{+\cdot}$ contaminant appeared at only 6% of the $SO^{+\cdot}$ ion signal. In Fig. 2(a), the appearance of an imbalance in the ion signal as a function of acetone flow is due to the rapid further reactions of the primary products, forming higher-mass products which were not monitored. Contributions to the ion spectrum due to the reactions of $O_2^{+\cdot}$ were accounted for using data available in the literature [23,24]. Percentages of products originating from the $SO^{+\cdot}$ reaction alone are plotted in Fig. 2(b). The two minor products from this reaction are not shown, for the sake of clarity (see Table 1). Nascent product distributions were obtained by extrapolating to zero flow, which indicates three major primary products in Fig. 2(b), as well as a secondary product, $C_3H_7O^+$, or protonated acetone.

3. Results and discussion

Rate coefficients, $k_{exp}^{(2)}$, and fractional product distributions, *f*, for the reactions of $SO^{+\cdot}$ and the supplementary reactions of $S_2^{+\cdot}$ and $O_2^{+\cdot}$ measured in the present study are presented in Table 1. Capture rate coefficients, $k_{th}^{(2)}$, calculated from the parameterized variational "transition state" theory of Su and Chesnavich [37] are presented for comparison with the experimentally-determined rate coefficients. Electric dipole polarizabilities and electric dipole moments for these calculations were obtained from standard reference sources [32,38]. All except 5 of the 23 reactions studied proceed at the theoretical capture rate, within experimental uncertainty. Of those 5, the reactions of $S_2^{+\cdot}$ with C_2H_2 and of $SO^{+\cdot}$ with CH_4 do not proceed; upper-limit values for the experimental rate coefficients are given, and no reaction products attributable to those reactions are observed. The reaction of $O_2^{+\cdot}$ with CH_4, which has also been measured previously [5,6], is quite slow at room temperature, and the reactions of $SO^{+\cdot}$ with OCS and with CH_2O are somewhat less than 50% efficient. Note that the slowest reactions are with the species of lowest atomicity, albeit the reactions of $SO^{+\cdot}$ and $O_2^{+\cdot}$ with C_2H_2 are quite fast (see Table 1).

Although the only signals detected in SIFT experiments are ion counts at various *m/z* values, the spatially resolved chemical environment of a fast flow reactor, the extremely low ion density, and the low level of overall excitation (e.g. no discharges are present in the reaction region) permit the unequivocal assignment of ion products in most situations. Indeed, in the present study, the empirical identities of the ion products are given with confidence, although the precise isomeric forms are not identified and must be inferred. Moreover, although the neutral products are not detected, with the $SO^{+\cdot}$ reactions the energetics usually constrains these to only one or at most a few possibilities. Table 1 indicates enthalpies of reaction, calculated from data available in standard thermochemical databases [11,39] (except as noted in the following), assuming formation of the products indicated. Note that the calculated enthalpy of reaction is rarely large enough to dissociate the neutral product(s) indicated, and therefore the ion/molecule reactions of $SO^{+\cdot}$ do not lead to fragmentation so much as to bond rearrangement. The same is not generally the case with the $O_2^{+\cdot}$ reactions (see Table 1).

Although numerous product channels are reported in several of the reactions of $SO^{+\cdot}$ and $O_2^{+\cdot}$ with the molecules in this study, note that the top two or three channels account for the majority, usually the overwhelming majority, of products in every case (see Table 1). Furthermore, the existence of products reported with $<5\%$ abundance should be regarded as somewhat uncertain, although they are generally consistent with the observed reactive behavior of these ions, and there is no *a priori* reason to exclude them from the product spectra. The reactions of $SO^{+\cdot}$ are discussed immediately in Sec. 3.1, especially in light of the interesting radical species generated, which have rarely been observed directly in the gas phase. Then follows a discussion of the relative reactivities

Table 1
Reaction rate coefficients, $k_{exp}^{(2)}$, theoretical capture rate coefficients, $k_{th}^{(2)}$, fractional product distributions, f, ion and proposed neutral products, and calculated reaction enthalpies, ΔH_{rxn}, for the reactions of $XY^{+\cdot}$ (X, Y = S, O) with the indicated neutral molecules investigated in the present study at 294.5 ± 2.5 K

Reactant	$k_{exp}^{(2)}$ ($cm^3\ s^{-1}$)	$k_{th}^{(2)}$ [a] ($cm^3\ s^{-1}$)	*f*	*m/z*	Ion product[b]	Neutral product[c]	ΔH_{rxn} [d] (kcal mol^{-1})
S_2^+ reactions							
C_2H_2 Acetylene	<5 (−12)	1.1 (−9)	...	...	no reaction	...	...
SO^+ reactions							
CH_4 Methane	<3 (−13)	1.1 (−9)	...	...	no reaction	...	...
C_2H_6 Ethane	1.3 (−9)	1.1 (−9)	0.80	50	$HSOH^+$	C_2H_4	−18
			0.20	29	$C_2H_5^+$	HSO	−9
C_3H_8 Propane	1.4 (−9)	1.2 (−9)	0.98	43	$C_3H_7^+$	HSO	−28
			0.02	50	$HSOH^+$	*n*-C_3H_6	−20
C_2H_2 Acetylene	1.2 (−9)	1.1 (−9)	0.60	46	CH_2S^+	CO	−79
			0.22	45	HCS^+	HCO	−39
			0.17	42	CH_2CO^+	S	−16
			0.01	29	HCO^+	HCS	−23
C_2H_4 Ethene	1.1 (−9)	1.1 (−9)	0.60	47	CH_2SH^+	HCO	−35
			0.20	46	CH_2S^+	CH_2O	−39
			0.06	31	CH_2OH^+	HCS	−7
			0.04	59	CH_3CS^+	HO	−38
			0.04	45	HCS^+	CH_2OH	−10
			0.02	50	$HSOH^+$	C_2H_2	−9
			0.02	48[e]	CH_3SH^+	CO	−65
			0.01	29	HCO^+	CH_3S	−24
			0.01	76	$SO^+ \cdot C_2H_4$	...	...
C_3H_4 Allene	1.2 (−9)	...	0.57	40	$C_3H_4^+$	SO	−14
			0.15	45	HCS^+	CH_3CO	−44
			0.07	59	CH_3CS^+	HCO	−70
			0.06	46	CH_2S^+	CH_2CO	−56
			0.06	43	CH_3CO^+	HCS	−53
			0.04	42	CH_2CO^+	CH_2S	−49
			0.03	39	$C_3H_3^+$	HSO	−33
			0.02	29	HCO^+	CH_3CS	...
C_3H_6 Propene	1.3 (−9)	1.3 (−9)	0.64	41	$C_3H_5^+$	HSO	−24
			0.14	42	$C_3H_6^+$	SO	−13
			0.13	29	$C_2H_5^+$	HS + CO	−21
			0.04	73	$C_3H_5S^+$	HO	...
			0.02	43	CH_3CO^+	CH_3S	−13
			0.02	45	HCS^+	C_2H_5O	−14
			0.01	72	$C_3H_4S^+$	H_2O	...
CH_3OH Methanol	2.2 (−9)	2.1 (−9)	0.90	31	CH_2OH^+	HSO	−25
			0.10	50	$HSOH^+$	CH_2O	−30

(*continued*)

Table 1 (*continued*)

Reactant	$k_{exp}^{(2)}$ ($cm^3\ s^{-1}$)	$k_{th}^{(2)}$ [a] ($cm^3\ s^{-1}$)	*f*	*m/z*	Ion product[b]	Neutral product[c]	ΔH_{rxn}[d] (kcal mol^{-1})
C_2H_5OH	2.3 (−9)	2.1 (−9)	0.65	29	$C_2H_5^+$	HOSO	−25
Ethanol			0.15	66	$HOSOH^+$	C_2H_4	...
			0.15	45	$C_2H_5O^+$	HSO	−50
			0.05	31	CH_2OH^+	CH_3SO	−5
CH_3OCH_3	1.8 (−9)	1.7 (−9)	0.90	45	$CH_3OCH_2^+$	HSO	−44
Dimethyl ether			0.10	46	$CH_3OCH_3^+$	SO	−6
OCS	4.9 (−10)	1.3 (−9)	0.55	64	S_2^+	CO2	−52
Carbonyl sulfide			0.45	80	S_2O^+	CO	~0
CH_2O	1.3 (−9)	2.7 (−9)	0.50	29	HCO^+	HSO	−20
Formaldehyde			0.49	50	$HSOH^+$	CO	−49
			0.01	78	$SO^+{\cdot}CH_2O$	...	...
CH_3CHO	3.0 (−9)	2.9 (−9)	1.00	43	CH_3CO^+	HSO	−46
Acetaldehyde							
$CH_3C(O)CH_3$	2.8 (−9)	2.9 (−9)	0.45	58	$CH_3C(O)CH_3^+$	SO	−14
Acetone			0.36	41	$C_3H_5^+$	HOSO	−19
			0.15	43	CH_3CO^+	CH_3SO	−23
			0.02	42	$C_3H_6^+$	SO_2	−29
			0.02	29	$C_2H_5^+$	HSO + CO	−4
HCOOH	1.5 (−9)	1.7 (−9)	0.85	66	$HOSOH^+$	CO	...
Formic acid			0.10	29	HCO^+	HOSO	−9
			0.05	50	$HSOH^+$	CO_2	−54
$HCOOCH_3$	2.1 (−9)	2.0 (−9)	0.55	31	CH_2OH^+	HSO + CO	−13
Methyl formate			0.30	80	CH_3OSOH^+	CO	...
			0.15	50	$HSOH^+$	CH_2O + CO	−18
O_2^+ reactions							
CH_4	5.8 (−12)	1.3 (−9)	1.00	47	$CH_3O_2^+$	H	...
Methane							
C_2H_2	1.3 (−9)	1.2 (−9)	0.85	26	$C_2H_2^+$	O_2	−15
Acetylene			0.10	42	CH_2CO^+	O	−63
			0.05	29	HCO^+	H + CO	−101
C_3H_4	1.3 (−9)	...	0.94	40	$C_3H_4^+$	O_2	−55
Allene			0.04	39	$C_3H_3^+$	HO_2	−67
			0.02	42	CH_2CO^+	CH_2O	−140
C_3H_6	1.5 (−9)	1.5 (−9)	0.50	42	$C_3H_6^+$	O_2	−54
Propene			0.37	29	$C_2H_5^+$	HO + CO	−80
			0.06	41	$C_3H_5^+$	HO_2	−57
			0.02	28	$C_2H_4^+$	HCOOH	−119
			0.02	45	$C_2H_5O^+$	H + CO	−119
			0.02	31	CH_2OH^+	CH_3CO	−115
			0.01	44	CH_3COH^+	CH_2O	−113

(*continued*)

Table 1 (*continued*)

Reactant	$k_{exp}^{(2)}$ ($cm^3\ s^{-1}$)	$k_{th}^{(2)}$ [a] ($cm^3\ s^{-1}$)	*f*	*m/z*	Ion product[b]	Neutral product[c]	ΔH_{rxn} [d] (kcal mol^{-1})
CH_3OCH_3	1.8 (−9)	1.9 (−9)	0.75	45	$CH_3OCH_2^+$	HO_2	−77
Dimethyl ether			0.25	46	$CH_3OCH_3^+$	O_2	−47
HCOOH	1.8 (−9)	1.9 (−9)	0.53	45	HCO_2^+	HO_2	−45
Formic acid			0.35	34	HO_2H^+	CO_2	−16
			0.07	46	$HCOOH^+$	O_2	−17
			0.05	29	HCO^+	HO_3	...

[a] Theoretical capture rate coefficients were calculated from the variational transition state theory of Su and Chesnavich [37], using electric dipole moments and electric dipole polarizabilities available from standard reference sources [32,38].

[b] The empirical form (i.e. atomic constituency) of the ion product is unequivocal in all except a very few cases [e.g. $C_2H_5^+$ (*m/z* = 29) could conceivably be HCO^+ (*m/z* = 29) in the reaction of $SO^{+\cdot}$ with C_3H_6 (propene)]. The indicated isomeric form of the ion is assumed for the calculation of reaction energetics using information available in standard databases [11,39] (except where noted in the text).

[c] The neutral products indicated are assumed for the calculation of reaction energetics using information available in standard databases [11,39] (except where noted in the text). See the text for further discussions on the expected neutral products which are not directly observed and must be inferred.

[d] Negative reaction enthalpies, ΔH_{rxn}, indicate exothermic reactions. The enthalpies indicated are calculated using the assumed isomeric forms of the ion and neutral products (see footnotes b and c) and information from standard databases [11,39] (except where noted in the text).

[e] The ∼2% product, $CH_3SH^{+\cdot}$, occurs at the same *m/z* (=48) as the parent ion, $SO^{+\cdot}$. After correction for the isotopic contributions of $^{12}CH_2{}^{34}S^{+\cdot}$, $^{12}CH_2{}^{33}SH^+$, and $^{13}CH_2{}^{32}SH^+$, the signal at *m/z* = 48 still levels out at ∼2% of the initial $SO^{+\cdot}$ signal in the rate-decay plot, implying formation of $CH_3SH^{+\cdot}$ as a reaction product.

of the $XY^{+\cdot}$ (X, Y = S, O) family of molecules (see Table 2), which show a number of systematic similarities and differences related to the relative recombination energies of these species, and to the strong polarity of $SO^{+\cdot}$ as opposed to $S_2^{+\cdot}$ and $O_2^{+\cdot}$. Finally, the implications of the $SO^{+\cdot}$ reactivity observed in this study for its chemistry in ISC are briefly discussed.

3.1. Reactions of $SO^{+\cdot}$

Charge transfer ("CT" in Table 2) is possible in just a few cases presented here for $SO^{+\cdot}$, and is the dominant product only in the reactions with allene (CH_2CCH_2) and acetone [$CH_3C(O)CH_3$]. Charge transfer is not observed where it is endothermic, even just slightly so (i.e. with ethene and ethanol; see Table 2), which implies that the $SO^{+\cdot}$ is in indeed in its ground $X\ ^2\Pi_r$ electronic state, as expected (see Sec. 2). Hydride (H^-) abstraction ("HAb" in Table 2) is much more prevalent than charge transfer, and may lead to the formation of either the thioperoxy radical, $HSO^{\cdot}$, or its structural isomer, $SOH^{\cdot}$. There has been considerable controversy over the enthalpies of formation of these two radicals [40], although Xantheas and Dunning have made a high-level ab initio study of the potential energy surface connecting the isomers and the dissociation channel leading to $H(^2S)$ + $SO(^3\Sigma^-)$ [41]. They computed values of -6.1 ± 1.3 and -0.7 ± 1.3 kcal mol^{-1} for $\Delta H_f^{\circ 298}$ ($HSO^{\cdot}$) and $\Delta H_f^{\circ 298}$ ($SOH^{\cdot}$), respectively, and a barrier of 46.3 kcal mol^{-1} for the isomerization $HSO^{\cdot} \leftrightharpoons SOH^{\cdot}$. They also computed a dissociation limit to $H(^2S)$ + $SO(^3\Sigma^-)$ of 56.2 kcal mol^{-1} above the ground state of $HSO^{\cdot}$ and 53.2 kcal mol^{-1} above that of $SOH^{\cdot}$ [41]. Thus, where $HSO^{\cdot}$ is indicated as the neutral product in Table 1, the calculated reaction exothermicity is never sufficient to dissociate the $HSO^{\cdot}$ into H + SO (dissociation to $HS^{\cdot}$ + O is a higher-energy process [41]). Moreover, there is enough reaction enthalpy to drive the isomerization in only a few cases. Therefore it may generally be concluded that the neutral products are formed "locked in" as $HSO^{\cdot}$ or $SOH^{\cdot}$. Which of these isomers is actually formed, if not both, is a matter for conjecture. However, the polarity of $SO^{+\cdot}$ makes the sulfur terminus more electrophilic than the oxygen: a recent ab initio study at the cc-pVTZ/CCSD(T) level of theory indicates a Mulliken popu-

lation of 0.693 on the S atom and 0.307 on the O atom of $SO^{+\cdot}$ [13,42]. Hence, the S-terminus rather than the O-terminus should initiate bonding interactions with the hydrogen leading to H^- abstraction in the majority of cases. Furthermore, the higher enthalpy of formation of $SOH^{\cdot}$ with respect to $HSO^{\cdot}$ reflects the lower hydride affinity of the O-terminus of $SO^{+\cdot}$ as compared with the S-terminus. Therefore we expect that $HSO^{\cdot}$ is the neutral product formed in the majority of cases, if not exclusively, and we have assumed formation of $HSO^{\cdot}$ in calculating the reaction enthalpies indicated in Table 1.

The $HSO^{\cdot}/SOH^{\cdot}$ appears in protonated form (empirically, $H_2SO^{+\cdot}$) in several reactions of $SO^{+\cdot}$ in the present study (i.e. with ethane, propane, ethene, methanol, formaldehyde, formic acid, and methyl formate; see Table 1). The lowest-energy forms of this ion are the *trans* and *cis* isomers of the hydrogen thioperoxide molecular ion, $HSOH^{+\cdot}$, with enthalpies of formation ($\Delta H_f^{\circ 298}$) of 188 and 190 kcal mol^{-1}, respectively, as estimated using a focal point extrapolation based on the cc-pVTZ/CCSD(T) level of ab initio theory [42]. We have used the estimated $\Delta H_f^{\circ 298}$ of the *trans* isomer to calculate the reaction enthalpy where $HSOH^{+\cdot}$ occurs in Table 1. The sulfoxide isomer, H_2SO^+, lies about 31 kcal mol^{-1} above the *trans*-$HSOH^+$ isomer [13,42], and hence, is unable to form in most cases where $HSOH^{+\cdot}$ appears in Table 1. The thiooxonium ylide, $H_2OS^{+\cdot}$, is intermediate in energy [42], but note that if reaction proceeds mechanistically by an initial hydride abstraction, followed by an internal proton transfer in the activated complex, $H_2OS^{+\cdot}$ is not likely to be an important isomeric product, since, as discussed above, the hydride transfer should initially form $HSO^{\cdot}$ in most cases; a proton transfer would then form *trans*- or *cis*-$HSOH^{+\cdot}$ or the unlikely higher-energy $H_2SO^{+\cdot}$. Very few experimental observations of the [2H, S, O] family of molecules have been reported [42,43].

$SO^{+\cdot}$ is also observed to abstract larger functional groups, formally speaking, i.e. OH^-, CH_3^-, and OCH_3^- (see Table 1). In its reactions with ethanol, acetone, and formic acid, ion products, which imply the formation of the hydroxysulfinyl radical, $HOSO^{\cdot}$, as the neutral product are observed; with ethanol and formic acid, the protonated form, $HOSOH^{+\cdot}$, also appears in a separate product channel (see Table 1). Laakso et al. [44] have computed the enthalpies of formation ($\Delta H_f^{\circ 298}$) of the four doublet radicals $HSOO^{\cdot}$, syn-$HOSO^{\cdot}$, $HSO_2^{\cdot}$, and anti-$HOOS^{\cdot}$ using the GAUSSIAN-2 methodology, and obtained values of 26.6, −57.7, −33.8, and 14.1 kcal mol^{-1}, respectively. We have used the value indicated for $\Delta H_f^{\circ 298}$ (syn-$HOSO^{\cdot}$) to calculate the reaction enthalpies where $HOSO^{\cdot}$ appears as a neutral product in Table 1. The resulting reaction exothermicities for these channels in the acetone and formic acid reactions mandate unequivocally that $HOSO^{\cdot}$ is the only isomer which can be formed. With ethanol, formation of the hydrogensulfonyl radical, $HSO_2^{\cdot}$, is barely exothermic (i.e. by ~0.6 kcal mol^{-1}) using the Laakso et al. values [44], but formation of $HOSO^{\cdot}$ is substantially exothermic (i.e. by 25 kcal mol^{-1}; see Table 1) and mechanistically simpler to explain. The abstraction of oxygen-containing groups in the reactions of $SO^{+\cdot}$ would logically be initiated by overlap of the electron-deficient sulfur terminus of the singly occupied $3\pi^1$ molecular orbital (SOMO) of $SO^{+\cdot}$ with one of the electron-rich, essentially nonbonding lone-pair orbitals (NBO) centered on the oxygen atom in the neutral molecule (i.e. a polar interaction between the δ^+ S atom of $SO^{+\cdot}$ and the δ^- O atom of the neutral molecule). In the reaction with ethanol, for example, a simple heterolytic cleavage would then result in a neutral fragment with the connectivity HO–S–O, rather than O–S(H)–O. The same mechanism would apply to the reaction with formic acid, although this is clearly not possible with the acetone reaction. Thus, the formation of $HOSO^{\cdot}$ (which is energetically mandated) in the reaction with acetone must proceed by the initial SOMO/NBO interaction, followed by a transfer of $H^{\cdot}$ or H^- from one of the methyl groups of acetone. The synthesis in the gas phase of neutral HOSOH and $HOSO^{\cdot}$ have recently been reported [45,46].

Note that the protonated form, $HOSOH^{+\cdot}$, does not appear in the reaction with acetone, and also that its contribution to the product spectrum is anti-correlated with the proton affinity (*PA*) of the leaving partner: i.e. $HOSOH^{+\cdot}$ is an 85% product channel in the reaction with HCO_2H, where CO (*PA* = 142 kcal

mol^{-1}) is the leaving partner; it is only a 15% product channel with C_2H_5OH, where C_2H_4 (PA = 163 kcal mol^{-1}) is the leaving partner; and it does not appear at all with $CH_3C(O)CH_3$, where C_3H_4 (e.g. PA = 179 kcal mol^{-1} for CH_3CCH) is the nominal leaving partner (PA values are taken from [47]). Such an anticorrelation of the protonated radical product channel is also observed with the H^- abstractions of $SO^{+\cdot}$ in the present study (see Tables 1 and 2) and with the H^- abstractions of $S_2^{+\cdot}$ from our previous studies [12,15,16]. This behavior implies a two-step mechanism whereby a heterogenic abstraction of H^- or OH^- is followed by an intramolecular proton transfer to the leaving radical when it has a PA comparable to, or greater than, its leaving partner (designated "HAb + P" for H^- abstraction and "HOAb + P" for OH^- abstraction in Table 2). The proton transfer may have a significant internal barrier in some cases, as, for example in the reaction of $SO^{+\cdot}$ with formaldehyde, where the formyl cation, HCO^+, appears as a product channel 50% of the time, even though CO has a much lower PA than $HSO^{\cdot}$ or $SOH^{\cdot}$ [12,42].

Formation of $CH_3SO^{\cdot}$ or one of its structural isomers is implied in two minor product channels in the reactions of $SO^{+\cdot}$, i.e. in a 5% channel with ethanol and a 15% channel with acetone (see Table 1). The thermochemistry of $CH_3SO^{\cdot}$ is poorly known, and we have adopted a value of $\Delta H_f^{\circ 298}(CH_3SO^{\cdot}) \sim$ 6 kcal mol^{-1} [48] for the reaction enthalpy calculations in Table 1. $CH_3SO^{\cdot}$ is thought to be an important reactive intermediate in the chemistry of atmospheric sulfur [49]. In the reaction of $SO^{+\cdot}$ with methyl formate, a 30% product channel leads most likely to the formation of the protonated methoxysulfinyl radical, $CH_3OSOH^{+\cdot}$ (see Table 1). Although the precise isomeric form of the product was not determined in these experiments, this reaction channel of $SO^{+\cdot}$ with HCO_2CH_3 is expected to be mechanistically similar to that leading to $HOSOH^+$ in the reaction with HCO_2H (see previous discussion). The neutral radical, $CH_3OSO^{\cdot}$, has been computed to be substantially lower in energy than its structural isomers, $CH_3SO_2^{\cdot}$ [50] and $CH_3SOO^{\cdot}$ [51]. Neutral $CH_3OSO^{\cdot}$ has been detected in solution by electron spin resonance spectroscopy [52], but its detection in the gas phase as a protonated species has not been reported previously.

In the reactions of $SO^{+\cdot}$ discussed above, the predominant mechanism (excluding charge transfer) appears to be a heterogenic abstraction in which a group R^- (R = H, OH, CH_3, OCH_3) is transferred to the sulfur terminus of the $SO^{+\cdot}$ molecular ion; intramolecular proton transfer frequently occurs before dissociation of the activated complex, in which case the SO-containing radical re-emerges as a charged (i.e. protonated) species. The reactions with small, unsaturated hydrocarbons (i.e. with acetylene, ethene and, to a lesser extent, allene and propene) show a dramatic departure from this pattern; with these, many product channels appear, most of which indicate major bonding rearrangements in the activated complex. Rupture of the S–O bond is commonplace here, whereas elsewhere in the present study it only occurs in the atom-switching channel with OCS to form $S_2^{+\cdot}$ and CO_2 (see Table 1). In the reactions $SO^{+\cdot} + C_2H_2$ and $SO^{+\cdot} + C_2H_4$, for example, the two dominant product channels are completely analogous, showing a rearrangement of the skeletal bonding to form $H_{n/2+k}CS^+ + H_{n/2-k}CO$, where n is the total number of hydrogen atoms, $k = 1$ for the dominant channel, and $k = 0$ for the secondary channel. These channels in C_2H_2 and C_2H_4 appear to be mechanistically identical for respective values of k. With allene, which has a three-carbon skeleton, product channels such as $H_{2-k}CS^+ + H_{2+k}C_2O$ and $H_{2+k}C_2S^+ + H_{2-k}CO$ are observed, where $k = 1$ is again more prevalent than $k = 0$ (see Table 1). The condition $k = 1$ indicates the occurrence of an H-atom migration in the activated complex, and therefore products showing such a migration are favored over products in which a hydrogen does not migrate. Product channels in which the charge appears on the oxygen-bearing group, e.g. $H_{2+k}CO^+ + H_{2-k}CS$ (k = 0, 1) in the reaction with C_2H_4, are observed in some cases, but with much lower prevalence than the analogous channels with sulfur-bearing ions (see Table 1); this reflects the initially greater localization of charge on the S-terminus of $SO^{+\cdot}$. A few other product channels are observed where S–O bond cleavage occurs, but the entire carbon skeleton of the hydrocarbon remains

associated with one of these atoms; notable among these is the very unusual 17% channel in the reaction with C_2H_2 forming $C_2H_2O^{+\cdot}$ (assumed to be the ketene molecular ion in Table 1) and atomic S; the analogous channel is also observed in the reaction with $O_2^{+\cdot}$. Hydride abstraction, so prevalent in many other reactions of $SO^{+\cdot}$, is only a very minor contribution to the reactivity with C_2H_4 and with CH_2CCH_2 (see Table 1).

The dominant reaction channels of $SO^{+\cdot}$ with small, unsaturated hydrocarbons, where the product ion contains either a C–S or a C–O bond, most likely proceed via a four-center intermediate, because energetics necessitate the respective formation of a C–O, or a C–S bond in the neutral product, and thus, after rupture of the S–O bond, the S atom and the O atom must pair with different C atoms. However, the rate coefficient for the reaction is at the collisional value (see Table 1), implying that there is no dependence on the input trajectory; furthermore, collisional association products are almost nonexistent (≤1%). This implies that the binary reaction occurs on a timescale shorter than ~200 ns, i.e. the average time between collisions with a He third-body under our experimental conditions. Thus, whatever the input trajectory, the interacting species must "lock" together and rapidly find the appropriate four-center configuration. Such locking is facilitated by the interaction between the $3\pi^1$ SOMO of $SO^{+\cdot}$ and the π-HOMO (highest order molecular orbital) of the hydrocarbon. That this interaction is strong is demonstrated by the analogous reactions of $S_2^{+\cdot}$, where the corresponding binary channels are generally endothermic, and three-body association is prominent (see Table 2).

3.2. Comparison of the reactivities of $XY^{+\cdot}$ (X, Y = S, O) molecular ions

The rate coefficients, ion products, and product branching fractions for the reactions of $S_2^{+\cdot}$, $SO^{+\cdot}$, and $O_2^{+\cdot}$ with the 16 neutral molecules in the present study are compared in Table 2, with data taken from the present and previous [5,6,15–25] studies. Also indicated (in parentheses) are the first ionization energies (*IE*s) of the neutral molecules, as well as the recombination energies (*RE*s) of the ions. Note that $O_2^{+\cdot}$ has a *RE* significantly higher than all the *IE*s except that of CH_4. Conversely, $S_2^{+\cdot}$ has a *RE* substantially lower than all these *IE*s. That of $SO^{+\cdot}$ lies in between, but is only greater than five of the neutral *IE*s. The difference $RE(I^+) - IE(M)$ in a reaction between an ion I^+ and a neutral molecule M can have a strong governing influence on the rate coefficient for that reaction, and on which product channels are competitive. This is amply demonstrated by the rapid reactions of atomic $S^+(^4S)$ with 34 organic molecules, including most of those in the present study, which in addition to a variety of competitive reaction channels show a very strong positive correlation of charge transfer prominence with charge transfer exothermicity [12,53]. $S^+(^4S)$ has a recombination energy (10.36 eV) very close to that of $SO^{+\cdot}(X\ ^2\Pi_r)$ (10.29 eV), and thus, the reactivities of these two ions might be expected to be similar. This is just what is observed [53].

It can be seen from Table 2 that the *RE*s of $XY^{+\cdot}$ (X, Y = S, O) have a powerful effect on their overall reactivities. For example, $S_2^{+\cdot}$ is by far the least reactive of the three ions: with six of the molecules it has either no reaction or it reacts simply by ternary (collisionally stabilized) association. With two more molecules, i.e. with allene and propene, association is ≥60% of the observed product. Where it does have binary reactions, the rate coefficients more often are smaller than the theoretical gas-kinetic rate coefficient, in contrast with the analogous reactions of $SO^{+\cdot}$ and $O_2^{+\cdot}$ (see Table 2). Note that hydride (H^-) abstraction to form $HS_2^{\cdot}$ and H^- abstraction with internal proton transfer to form $HS_2H^{+\cdot}$ are by far the most prevalent binary reactions of $S_2^{+\cdot}$. Although it is clear that $S_2^{+\cdot}$ has a strong propensity for H^- abstraction, comparison of $\Delta H_f^{\circ 298}(XY^{+\cdot}) - \Delta H_f^{\circ 298}(HXY^{\cdot})$ for the three ions (X, Y = S, O), which is an approximate but unequivocal measure of their relative hydride affinities (*HA*s), shows a progression in the order $HA(S_2^{+\cdot}) < HA(SO^{+\cdot}) < HA(O_2^{+\cdot})$ (thermodynamic data necessary for this consideration are available in references cited heretofore [11,15,39,41]). Conversely, the proton affinities (*PA*s) of the neutral hydrides [12,15,42,47] progress in the reverse order: $PA(HS_2^{+\cdot}) > PA(HSO^{\cdot}) > PA(HO_2^{+})$. Thus, we should expect that H^- abstraction will occur with

Table 2
Comparison of the reactivities of the $XY^{+\cdot}$ (X, Y = S, O) diatomic cations with the organic molecules selected for the present study; recombination energies of the ions (in eV) and first ionization energies of the neutral molecules (in eV) are indicated in parentheses below the corresponding reactant; also indicated are product percentages (%) for each product channel and experimentally measured bimolecular rate coefficients ($k_{exp}^{(2)}$) for each reaction

Reactant	%	S_2^+ (9.36)	$k_{(2)}^{exp}$ [b]	%	SO^+ [a] (10.29)	$k_{(2)}^{exp}$ [b,c]	%	O_2^+ [a] (12.07)	$k_{exp}^{(2)}$ [b]
CH_4 (12.51)		NR	··· [17]		NR	<3 (−13)	100	$CH_3O_2^+$	5.8 (−12) [t.w.]
C_2H_6 (11.52)	100	HAb + P	3.2 (−11) [16]	80 20	HAb + P HAb	1.3 (−9)	100	CT	1.2 (−9) [25]
C_3H_8 (10.95)	90 10	HAb HAb + P	9.9 (−10) [16]	98 2	HAb HAb + P	1.4 (−9)	100	CT	1.4 (−9) [25]
C_2H_2 (11.40)		NR	<5 (−12) [t.w.]	60 22 17 1	CH_2S^+ HCS^+ CH_2CO^+ HCO^+	1.2 (−9)	85 10 5	CT CH_2CO^+ HCO^+	1.3 (−9) [t.w.]
C_2H_4 (10.51)	100	AS	6.4 (−11)[d] [16]	60 20 6 4 4 2 2 1 1	CH_2SH^+ CH_2S^+ CH_2OH^+ CH_3CS^+ HCS^+ HAb + P CH_3SH^+ HCO^+ AS	1.1 (−9)	100	CT	6.8 (−10) [5]
CH_2CCH_2 (9.69)	65 20 5 5 5	AS CS_2^+ $C_3H_3S^+$ CH_3CS^+ CH_2CS^+	1.0 (−9)[d] [16]	57 15 7 6 6 4 3 2	CT HCS^+ CH_3CS^+ CH_2S^+ CH_3CO^+ CH_2CO^+ HAb HCO^+	1.2 (−9)	94 4 2	CT HAb CH_2CO^+	1.3 (−9) [t.w.]
CH_2CHCH_3 (9.73)	60 15 10 5 5 5	AS $CH_2S_2^+$ $C_3H_4S^+$ CH_3CS^+ HAb $C_3H_5S^+$	1.2 (−9)[d] [16]	64 14 13 4 2 2 1	HAb CT $C_2H_5^+$ $C_3H_5S^+$ CH_3CO^+ HCS^+ $C_3H_4S^+$	1.3 (−9)	50 37 6 2 2 2 1	CT $C_2H_5^+$ HAb $C_2H_4^+$ $C_2H_5O^+$ CH_2OH^+ $C_2H_4O^+$	1.5 (−9) [t.w.]
CH_3OH (10.84)	90 8 2	HAb + P HAb $CH_2S_2^+$	8.8 (−10) [15]	90 10	HAb HAb + P	2.2 (−9)	50 50	CT HAb	1.0 (−9) [22]
C_2H_5OH (10.48)	100	HAb	2.2 (−9) [15]	65 15 15 5	HOAb HOAb + P HAb CH_2OH^+	2.3 (−9)	75 25	HAb CT	2.3 (−9) [22]

(*continued*)

Table 2 (*continued*)

Reactant	%	S_2^+ (9.36)	$k_{(2)}^{exp\ b}$	%	SO^+ [a] (10.29)	$k_{(2)}^{exp\ b,c}$	%	O_2^+ [a] (12.07)	$k_{exp}^{(2)\ b}$
CH_3OCH_3 (10.03)	100	HAb	1.6 (−9) [16]	90 10	HAb CT	1.8 (−9)	75 25	HAb CT	1.8 (−9) [t.w.]
OCS (11.13)	100	S_3^+	5.8 (−12) [5]	55 45	S_2^+ S_2O^+	4.9 (−10)	100	CT	1.2 (−9) [6]
CH_2O (10.88)	100	HAb + P	1.1 (−10) [15]	50 49 1	HAb HAb + P AS	1.3 (−9)	60 40	CT HAb	2.2 (−9) [23]
CH_3CHO (10.23)	100	HAb	2.2 (−9) [16]	100	HAb	3.0 (−9)	55 45	CT HAb	2.3 (−9) [23]
$CH_3C(O)CH_3$ (9.70)	100	AS	1.4 (−9)[d] [16]	45 36 15 2 2	CT HOAb CH_3CO^+ $C_3H_6^+$ $C_2H_5^+$	2.8 (−9)	60 40	CT CH_3CO^+	2.7 (−9) [23]
HCOOH (11.33)	100	AS	5.0 (−11)[d] [15]	85 10 5	HOAb + P HOAb HAb + P	1.5 (−9)	53 35 7 5	HAb HAb + P CT HOAb	1.8 (−9) [t.w.]
$HCOOCH_3$ (10.84)	100	AS	3.9 (−10)[d] [16]	55 30 15	CH_2OH^+ CH_3OSOH^+ HAb + P	2.1 (−9)	>95 <5	CH_2OH^+ CT	2.3 (−9) [20]

[a] Ion products are classified by reaction type as follows: AS = ternary association; CT = charge (i.e. electron) transfer; HAb = hydride (H^-) abstraction; HAb + P = hydride (H^-) abstraction followed by intramolecular proton (H^+) transfer; HOAb = hydroxide (OH^-) abstraction; HOAb + P = hydroxide (OH^-) abstraction followed by intramolecular proton (H^+) transfer; NR = no reaction; other ion products are given explicitly, in their assumed isomeric forms where possible.

[b] Experimentally determined binary rate coefficients are given in cm^3 $molecule^{-1}$ s^{-1}. Rate coefficients and product distributions for reactions not studied in the present work are taken from the references indicated in brackets immediately below the tabulated rate coefficients ([t.w.] = measured in the present work).

[c] All of the reactions of $SO^{+\cdot}$ shown here are from the present work.

[d] Rate coefficients for ternary association reactions are given as effective binary rate coefficients at ~0.5 Torr carrier pressure. For more details, see [15,16].

$SO^{+\cdot}$ and $O_2^{+\cdot}$ where it cannot occur with $S_2^{+\cdot}$, but that H^- abstraction with internal proton transfer will be more prevalent with $S_2^{+\cdot}$ than with $SO^{+\cdot}$, and more prevalent with $SO^{+\cdot}$ than with $O_2^{+\cdot}$. Indeed, this is exactly what is observed (see, e.g. the reactions with CH_2CHCH_3, CH_3OH, CH_2O, and HCOOH in Table 2), although the pattern is imperfectly represented in the data due to the alternative binary reaction channels available to $SO^{+\cdot}$ and $O_2^{+\cdot}$.

For $O_2^{+\cdot}$, charge transfer is highly competitive with other reaction channels in most cases. Only with CH_4, which has an *IE* (12.51 eV) higher than the *RE* of $O_2^{+\cdot}$ (12.07 eV), is charge transfer not observed, but it accounts for ≥50% of the product in 11 of the remaining 15 reactions (see Table 2). H^- abstraction can efficiently compete with charge transfer in some cases, and is the second most prevalent product in the reactions of $O_2^{+\cdot}$ [note that with methyl formate, HCO_2CH_3, where the principal product is CH_2OH^+, the neutral fragments are likely to be $HO_2^{\cdot}$ + CO, analogous to the expected products of the corresponding reaction of $SO^{+\cdot}$ (see Table 1)]. In the reaction of $O_2^{+\cdot}$ with formic acid, HCO_2H, a H^- abstraction followed by internal proton transfer is observed,

forming $HO_2H^{+\cdot}$ + CO_2, which was not reported by other workers [5,6,20]. We have no explanation for this difference. Intriguingly, the sum of the HAb and HAb + P channel percentages for this reaction (88%; see Table 2) agrees very well with the reported contribution from the H^- abstraction channel alone (90%) in a recent study by Španěl and Smith [20]. The appearance of a HAb + P channel in this reaction is entirely consistent with the general reactive behavior of these $XY^{+\cdot}$ (X, Y = S, O) ions as discussed above. Moreover, such a channel is expected, since $PA(HO_2^{\cdot}) > PA(CO_2)$ by ~29 kcal mol^{-1} [47]. The charge transfer channel percentage (7%) also agrees with the value found by Španěl and Smith (10%) [20]. Additionally, we observe a small (5%) hydroxide (OH^-) abstraction channel in this reaction, which was not reported previously [5,6,20]. OH^- abstraction is very rare with $O_2^{+\cdot}$, whereas it is not infrequent with $SO^{+\cdot}$, presumably reflecting the stronger polar interaction of $SO^{+\cdot}$ with the electron-rich oxygen on the neutral molecule. Thus, although $O_2^{+\cdot}$ certainly has enough recombination energy to drive OH^- abstraction, mechanistically it prefers other reaction channels, particularly charge transfer and H^- abstraction. Hydroxide abstraction has also been observed in a few reactions of $S_2^{+\cdot}$ (forming the $HOS_2^{\cdot}$ radical), i.e. with CH_3COOH, C_2H_5COOH, and 2-C_3H_7OH [15,16], although it does not occur with any of the molecules in the present study (see Table 2), and H^- abstraction is generally the more competitive process for $S_2^{+\cdot}$ reactions. With $SO^{+\cdot}$, conversely, OH^- abstraction is more prominent than H^- abstraction where they both occur (see Table 2).

The differences among $S_2^{+\cdot}$, $SO^{+\cdot}$, and $O_2^{+\cdot}$ in their reactions with the unsaturated hydrocarbons (C_2H_2, C_2H_4, CH_2CCH_2, and CH_2CHCH_3) are striking. Again, $O_2^{+\cdot}$ reactions are dominated by charge transfer, which constitutes the overwhelming majority of product except in the reaction with propene. $S_2^{+\cdot}$ is unreactive with acetylene, and ternary association dominates its reactions with ethene, allene, and propene. The dominant binary channels for $S_2^{+\cdot}$ with allene and propene are abstractions (with ethene loss) forming $CS_2^{+\cdot}$ and $CH_2S_2^{+\cdot}$, respectively; other binary product channels, indicating rupture of the S–S bond of $S_2^{+\cdot}$, are relatively minor (see Table 2). In the reaction of $O_2^{+\cdot}$ with CH_2CHCH_3, a small (2%) channel forming $C_2H_4^{+\cdot}$ is formally a CH_2^- abstraction, which may be analogous to the CH_2 abstraction in the $S_2^{+\cdot}$ reaction. Interestingly, such abstractions (with ethene loss) of C from CH_2CCH_2 and of CH_2 from CH_2CHCH_3 are entirely absent in the analogous reactions of $SO^{+\cdot}$. Instead, $SO^{+\cdot}$ much more extensively undergoes reactions that break the S–O bond as well as a C–C bond on the carbon skeleton, as discussed in Sec. 3.1. Similar reaction channels with $S_2^{+\cdot}$ and $O_2^{+\cdot}$ are observed in very few cases, and are always quite minor (see Table 2). Thus, such channels probably are facilitated mechanistically by the polar nature of $SO^{+\cdot}$, which the other two $XY^{+\cdot}$ (X, Y = S, O) ions lack.

3.3. Interstellar chemistry of $SO^{+\cdot}$

In the present study, the ion/molecule reactions of $SO^{+\cdot}$ are rapid in the majority of cases, being at or near the gas-kinetic limit. Where the neutral partners have permanent electric dipole moments, fast ion/molecule reactions are expected to be significantly faster at the low temperatures of interstellar molecular clouds (ISC) [54,55]. Therefore, depending on the chemical and physical features of the ISC of interest, it may not be sufficient to assume simply that electron/ion dissociative recombination is the only important destruction process for $SO^{+\cdot}$ [7,8]. It has been noted, for example, that in relatively hot ($T \sim 100$–200 K) clumps in star-forming molecular clouds, such as the "compact ridge" in the Orion KL cloud, complex interstellar organic molecules such as CH_3OH, CH_3OCH_3, HCO_2H, and HCO_2CH_3, whose reactions with $SO^{+\cdot}$ we have studied here, can reach quite high abundance levels [56].

Unsaturated hydrocarbons and other unsaturated carbon-containing molecules are abundant in the cold, dark Taurus Molecular Cloud (TMC-1), which is one of the most renowned "chemical factories" among ISC [57]. The present results show that the reactions of $SO^{+\cdot}$ with C_2H_2 and C_2H_4 couple the interstellar S–O and S–C chemistries, which have previously been considered to be largely decoupled [7,8]. Where molecules such as C_2H_2 and C_2H_4 reach high levels of

abundance, such reactions of $SO^{+\cdot}$ may be significant pathways to organosulfur compounds in ISC. Because hydride abstraction occurs in many reactions of $SO^{+\cdot}$, and most likely leads to the formation of the thioperoxy radical, $HSO^{\cdot}$ (see previous discussion), this radical should be included in searches for new gas phase species in ISC. The microwave spectrum of $HSO^{\cdot}$ has been recorded [58], although more detailed characterization of its microwave transitions may be necessary for interstellar searches.

4. Summary and conclusions

The reactions of the diatomic π-radical cation $SO^{+\cdot}$ with 16 molecules representing examples of several classes of organic compound have been studied with a SIFT and compared with the reactions of $S_2^{+\cdot}$ and $O_2^{+\cdot}$ with the same species.

Reactions of $SO^{+\cdot}$ are generally characterized by heterogenic bonding to form π-radical abstraction products such as $HSO^{\cdot}/SOH^{\cdot}$, $HOSO^{\cdot}$, $CH_3SO^{\cdot}$, and $CH_3OSO^{\cdot}$. Such products frequently appear in the ion product spectra in their protonated forms when the leaving partner (i.e. the leaving molecule) has a proton affinity lower than that of the radical. Charge transfer occurs when it is exothermic, although it is the majority channel only in the reaction with allene; abstraction channels effectively compete with charge transfer in the reactions with propene and acetone. Rupture of the S–O bond is indicated only in the reactions of $SO^{+\cdot}$ with small, unsaturated hydrocarbons, and in its reaction with OCS. These intimate reactions, where 2–3 bonds are generally broken, likely proceed through a four-center reaction intermediate.

The reactivities of the three isovalent ions $XY^{+\cdot}$ (X, Y = S, O) with the neutral molecules in the present study have been compared. A very strong correlation of the rate and the kind of reactivity with $RE(XY^{+\cdot}) - IE(M)$, i.e. the difference between the recombination energy of the ion and the first ionization energy of the neutral molecule, M, has been observed. When RE − IE is significantly greater than zero, (generally, >0.5 eV), charge transfer becomes a competitive, if not always dominant, binary reaction channel. Thus, charge transfer is the principal reaction channel for $O_2^{+\cdot}$ in the present study, which has the largest RE − IE of the three ions. Conversely, with $S_2^{+\cdot}$, which generally has a substantially negative RE − IE, charge transfer is not observed, three-body association is common, and reaction rate coefficients are generally smaller than for the other $XY^{+\cdot}$ (X, Y = S, O) ions. With its intermediate RE − IE, $SO^{+\cdot}$ most frequently combines rapid binary reaction with intimate reaction to form products with new bonding arrangements. Due to its polar nature, which is lacking in $S_2^{+\cdot}$ and $O_2^{+\cdot}$, $SO^{+\cdot}$ interacts more strongly with electron-rich alcohol and carbonyl oxygen atoms than its sister ions, and thus has a greater affinity for OH^- and other oxygen-containing functional groups.

The present study shows that $SO^{+\cdot}$ is rapidly destroyed in most of its reactions with small organic molecules. Where such molecules are abundant in ISC, models of the chemistry should take such reactions of $SO^{+\cdot}$ into account. Particularly with small, unsaturated hydrocarbons, $SO^{+\cdot}$ is observed to couple the S–O and S–C chemistries in ISC, which had previously been considered to be largely decoupled. The common abstraction products of $SO^{+\cdot}$ reactions, such as $HSO^{\cdot}$ (or its isomer, $SOH^{\cdot}$) and $HOSO^{\cdot}$, should be included in searches for new interstellar species. By revealing how certain transient species can be synthesized in the gas phase, studies such as the present one hopefully will stimulate gas-phase synthesis and further characterization of such species, which are of fundamental as well as practical interest to many branches of chemistry.

Acknowledgements

The National Science Foundation, Division of Astronomical Sciences, is gratefully acknowledged for funding this work under grant no. AST-9415485. The authors are extremely grateful to T. Daniel Crawford of the Center for Computational Quantum Chemistry at The University of Georgia for computing the dipole moment and Mulliken population of $SO^{+\cdot}$, as well as the enthalpies of formation of the various isomeric forms of $H_2SO^{+\cdot}$ using coupled cluster ab initio methods.

References

[1] U.J. Sofia, J.A. Cardelli, B.D. Savage, Astrophys. J. 430 (1994) 650.
[2] E. Herbst, Annu. Rev. Phys. Chem. 46 (1995) 27.
[3] A. Dalgarno, J. Chem. Soc., Faraday Trans. 89 (1993) 2111.
[4] D. Smith, Chem. Rev. 92 (1992) 1473.
[5] Y. Ikezoe, S. Matsuoka, M. Takabe, A. Viggiano, Gas Phase Ion Molecule Reaction Rate Constants Through 1986, Maruzen, Tokyo, 1987.
[6] V.G. Anicich, J. Phys. Chem. Ref. Data 22 (1993) 1469.
[7] B.E. Turner, Astrophys. J. 430 (1994) 727.
[8] M.C. McCarthy, Stellar Evolution, Stellar Explosions and Galactic Chemical Evolution, A. Mezzacappa (Ed.), IOP, Philadelphia, 1998, p. 205.
[9] B.E. Turner, Astrophys. J. 468 (1996) 694.
[10] J. Emsley, The Elements, Clarendon, Oxford, 1990.
[11] W.G. Mallard, P.J. Linstrom (Eds.), NIST Webbook, NIST Standard Reference Database Number 69, National Institute of Standards and Technology, Gaithersburg, MD, 1998, http://webbook.nist.gov.
[12] N.G. Adams, T.L. Williams, L.M. Babcock, B.K. Decker, Recent Res. Devel. Physical Chem. 3 (1999) 191.
[13] T.D. Crawford, private communication, a value of 2.3 ± 0.2 debye for the electric dipole moment of ground-state $SO^{+\cdot}$ appears in [9], from an unpublished personal communication.
[14] W.J. Chesnavich, T. Su, M.T. Bowers, J. Chem. Phys. 72 (1980) 2641.
[15] B.K. Decker, N.G. Adams, L.M. Babcock, Int. J. Mass Spectrom. 185/186/187 (1999) 727.
[16] B.K. Decker, N.G. Adams, Int. J. Mass Spectrom. Ion Processes 165/166 (1997) 257.
[17] T. Schindler, C. Berg, G. Niedner-Schatteburg, V.E. Bondybey, Ber. Bunsenges. Phys. Chem. 96 (1992) 1114.
[18] G. Niedner-Schatteburg, J. Silha, T. Schindler, V.E. Bondybey, Chem. Phys. Lett. 187 (1991) 60.
[19] P. Španěl, D. Smith, Int. J. Mass Spectrom. Ion Processes 172 (1998) 239.
[20] P. Španěl, D. Smith, Int. J. Mass Spectrom. Ion Processes 172 (1998) 137.
[21] S.T. Arnold, A.A. Viggiano, R.A. Morris, J. Phys. Chem. A 101 (1997) 9351.
[22] P. Španěl, D. Smith, Int. J. Mass Spectrom. Ion Processes 167/168 (1997) 375.
[23] P. Španěl, Y. Ji, D. Smith, Int. J. Mass Spectrom. Ion Processes 165/166 (1997) 25.
[24] P. Španěl, D. Smith, J. Chem. Phys. 104 (1996) 1893.
[25] S. Matsuoka, Y. Ikezoe, J. Phys. Chem. 92 (1988) 1126.
[26] N.G. Adams, D. Smith, Techniques for the Study of Ion–Molecule Reactions, J.M. Farrar, W.H. Saunders (Eds.), Wiley, New York, 1988, p. 165.
[27] K.P. Huber, G. Herzberg, Molecular Spectra and Molecular Structure IV. Constants of Diatomic Molecules, Van Nostrand Reinhold, New York, 1979.
[28] J.D. Lambert, Vibrational and Rotational Relaxation in Gases, Clarendon, Oxford, 1977.
[29] M. Tichy, A.B. Rakshit, D.G. Lister, N.D. Twiddy, N.G. Adams, D. Smith, Int. J. Mass Spectrom. Ion Phys. 29 (1979) 231.
[30] C.L. Yaws, Handbook of Viscosity, Library of Physico-Chemical Property Data, Gulf Publishing, Houston, 1995.
[31] W.D. Monnery, W.Y. Svrcek, A.K. Mehrotra, Can. J. Chem. Eng. 73 (1995) 3.
[32] D.R. Lide (Ed.), CRC Handbook of Chemistry and Physics, 78th ed., CRC, Boca Raton, FL, 1997.
[33] M.D. Taylor, J. Bruton, J. Am. Chem. Soc. 74 (1952) 4151.
[34] Specifically, the ratio of bulk ion velocity to bulk flow velocity was determined to be 1.51 for this particular SIFT apparatus, by measuring the flight times of ion pulses at known carrier flows.
[35] N.G. Adams, D. Smith, Int. J. Mass Spectrom. Ion Phys. 21 (1976) 349.
[36] N.G. Adams, D. Smith, J. Phys. B 9 (1976) 1439.
[37] T. Su, W.J. Chesnavich, J. Chem. Phys. 76 (1982) 5183.
[38] Lange's Handbook of Chemistry, 14th ed., J.A. Dean (Ed.), McGraw-Hill, New York, 1992.
[39] S.G. Lias, J.E. Bartmess, J.F. Liebman, J.L. Holmes, R.D. Levin, W.G. Mallard, NIST Positive Ion Energetics, Version 1.1, NIST Standard Reference Database 19A, National Institute of Standards and Technology, Gaithersburg, MD, 1990.
[40] A. Goumri, D. Laakso, J.-D.R. Rocha, C.E. Smith, P. Marshall, J. Chem. Phys. 102 (1995) 161.
[41] S.S. Xantheas, T.H. Dunning Jr., J. Phys. Chem. 97 (1993) 6616.
[42] B.K. Decker, N.G. Adams, L.M. Babcock, T.D. Crawford, H.F. Schaefer III, J. Am. Chem.
[43] M. Iraqi, H. Schwarz, Chem. Phys. Lett. 221 (1994) 359.
[44] D. Laakso, C.E. Smith, A. Goumri, J.-D.R. Rocha, P. Marshall, Chem. Phys. Lett. 227 (1994) 377.
[45] A.J. Frank, M. Sadilek, J.G. Ferrier, F. Turecek, J. Am. Chem. Soc. 118 (1996) 11321.
[46] A.J. Frank, M. Sadilek, J.G. Ferrier, F. Turecek, J. Am. Chem. Soc. 119 (1997) 12343.
[47] E.P.L. Hunter, S.G. Lias, J. Phys. Chem. Ref. Data 27 (1998) 413.
[48] F. Domine, T.P. Murrells, C.J. Howard, J. Phys. Chem. 94 (1990) 5839.
[49] G.S. Tyndall, A.R. Ravishankara, Int. J. Chem. Kinet. 23 (1991) 483.
[50] S.R. Davis, J. Phys. Chem. 97 (1993) 7535.
[51] M.L. McKee, Chem. Phys. Lett. 211 (1993) 643.
[52] B.C. Gilbert, C.M. Kirk, R.O.C. Norman, J. Chem. Res. (M) (1977) 1974.
[53] B.K. Decker, L.M. Babcock, N.G. Adams, J. Phys. Chem. A, in press.
[54] D.C. Clary, D. Smith, N.G. Adams, Chem. Phys. Lett. 119 (1985) 320.
[55] N.G. Adams, D. Smith, D.C. Clary, Astrophys. J. 296 (1985) L31.
[56] T.J. Millar, E. Herbst, S.B. Charnley, Astrophys. J. 369 (1991) 147.
[57] W.M. Irvine, P.F. Goldsmith, A. Hjalmarson, Interstellar Processes, D.J. Hollenbach, H.A. Thronson Jr. (Eds.), Reidel, Dordrecht, 1987, p. 561.
[58] Y. Endo, S. Saito, E. Hirota, J. Chem. Phys. 75 (1981) 4379.